Brigham Young University
BYU ScholarsArchive

All Faculty Publications

2003-03-01

Advances in Experimental Method and Analysis for Estimation of Geometrically-Necessary Dislocations

Brent L. Adams
b_l_adams@byu.edu

Bassem S. El-Dasher

See next page for additional authors

Follow this and additional works at: https://scholarsarchive.byu.edu/facpub

 Part of the Mechanical Engineering Commons

Original Publication Citation
Vopr. Materialoved , no. 1, pp. 49-54. Jan.-Mar. 23

BYU ScholarsArchive Citation

Adams, Brent L.; El-Dasher, Bassem S.; and Rollett, Anthony D., "Advances in Experimental Method and Analysis for Estimation of Geometrically-Necessary Dislocations" (2003). *All Faculty Publications*. 508.
https://scholarsarchive.byu.edu/facpub/508

This Peer-Reviewed Article is brought to you for free and open access by BYU ScholarsArchive. It has been accepted for inclusion in All Faculty Publications by an authorized administrator of BYU ScholarsArchive. For more information, please contact scholarsarchive@byu.edu.

Authors
Brent L. Adams, Bassem S. El-Dasher, and Anthony D. Rollett

This peer-reviewed article is available at BYU ScholarsArchive: https://scholarsarchive.byu.edu/facpub/508

ADVANCES IN EXPERIMENTAL METHOD AND ANALYSIS FOR ESTIMATION OF GEOMETRICALLY-NECESSARY DISLOCATIONS

B. S. El-Dasher[1], B. L. Adams[2] and A. D. Rollett[1]

[1]Carnegie Mellon University, Pittsburgh, PA 15213, USA
[2]Brigham Young University, Provo, UT 84602, USA

Abstract: Advances in experimental methods for determination of the geometrically-necessary dislocation (GND) tensor, based on electron backscattering diffraction, are described. Data are presented for directionally-solidified 99.999% Aluminum possessing a strong <001> columnar texture, with the primary focus being the interactions of the plastic deformation field with grain boundaries. Alternate methods of solving for the GND content are illustrated and compared. Implications of the observations for strain-gradient plasticity theory are discussed.

1. Introduction

Historically, experimental observation has shown that the constituent grains of polycrystalline materials develop complex patterns of heterogeneity over a wide range of length scales during plastic deformation. The classical theory of crystal plasticity, however, is limited to those interactions arising from the enforcement of mechanical compatibility [1]. It is evident that an understanding of the behavior of grain boundaries, and how they interact with deformation mechanisms as they change their structure to accommodate deformation, has been missing. These interactions are anticipated to set the necessary length scale(s) as discussed in the context of strain and gradient plasticity [2] and as seen clearly in the Hall-Petch relationship.

Recent work has shown that utilizing information obtained by electron backscattering diffraction (EBSD) and the use of Orientation Imaging Microscopy (OIM), which provides automated scanning measurements of the lattice orientation near grain boundaries may be a useful experimental technique to help provide this length scale. Computing the lattice curvature from these orientation measurements and consequently relating this curvature to estimates of the geometrically necessary dislocation (GND) density provides a promising experimental vehicle for the study of plasticity in crystalline materials [3]. The primary driving force behind the work presented here is to further exploit this experimental method by investigating the most reliable GND estimation method.

2. Theoretical

2.1. Basic Relationships

GND, from a continuum perspective, are the dislocations that are required to support a particular curvature in the crystallographic lattice at any given point in a deformed structure [4]. The fundamental equation of continuum dislocation theory establishes a link between the elastic distortion tensor β^e and the dislocation tensor α [5]:

$$\alpha = \operatorname{curl} \beta^e \ . \tag{1}$$

Relating the dislocation tensor to the curvature of the elastic strain and lattice orientation [3] yields the following simplified form:

$$\alpha_{ij} = e_{ikl}\left(\varepsilon^{e}_{jl,k} + g_{jl,k}\right) \tag{2}$$

where e_{ikl} are components of the permutation tensor, $\varepsilon^{e}_{jl,k}$ the infinitesimal elastic strain gradient, and $g_{jl,k}$ the gradient in lattice orientation. In the absence of long-range elastic stress fields, Nye's original formulation of the dislocation tensor is retrieved [6]:

$$\alpha_{ij} = e_{ikl} g_{jl,k} \tag{3}$$

Equation (3) then provides a direct relationship between the measured crystallographic orientation gradient and the dislocation tensor. Nye's work also highlighted a precise connection between the dislocation tensor and the local dislocation network:

$$\alpha_{ij} = \sum_{k=1}^{K} \rho^{k} \mathrm{b}_{i}^{k} \hat{\mathrm{z}}_{j}^{k} \tag{4}$$

where the sum is over all the dislocation types present in the material, ρ^{k} denotes the density of the dislocation of type k, and $\mathbf{b}^{k}$ and $\hat{\mathrm{z}}^{k}$ denote the Burger's vector and unit line direction of the specific dislocation type. Since Nye originally solved this relation for the trivial case of the dislocation systems of a simple cubic lattice, the mathematical problem posed was a system of nine linear equations with nine unknown densities.

Since the face-centered lattice of Aluminum presents twelve unique $\{111\}\langle 110\rangle$ slip systems, each with three dislocations (1 screw and 2 edge), application of equation (4) to this crystal lattice alters the problem to one of an underdetermined set of nine equations with thirty-six unknown densities. It is then evident that an appropriate method for solving this problem is needed. The next two subsections describe a previously illustrated method [3], which computationally relies on the simplex method of linear programming, as well as a more recently adapted method related to the Normal Equations.

2.2. Lower-bound fcc deconstruction

Since k in equation (4) describes the type of dislocation, and the term $\mathrm{b}_{i}^{k}\hat{\mathrm{z}}_{j}^{k}$ is simply the dyadic $\mathbf{b}^{k} \otimes \mathbf{z}^{k}$ (which provides the geometric definition of k) we can then define the set Δ that describes all the dislocations in the fcc lattice as follows:

$$\Delta = \left\{ \mathbf{b}^{1} \otimes \mathbf{z}^{1}, \mathbf{b}^{2} \otimes \mathbf{z}^{2}, \ldots, \mathbf{b}^{K} \otimes \mathbf{z}^{K} \right\} \quad \text{where } K=36 \tag{5}$$

Now, despite the underdetermined nature of the problem, we can consider only the set of nine dislocations, such that $\Delta' \subset \Delta$, that yield a 'lower bound' solution by coupling equation (4) with the following condition:

$$\textbf{minimum} \left\{ \rho_{\mathbf{GND}} = \sum_{k \in \Delta'} \rho^{k} \;\middle|\; \Delta' \subset \Delta, \alpha = \sum_{k \in \Delta'} \rho^{k} \mathbf{b}^{k} \otimes \hat{\mathbf{z}}^{k} \right\} \tag{6}$$

where ρ_{GND} is the sum of all individual dislocation densities. To computationally determine the set Δ', the Simplex method [7] is carried out with the sum of all the dislocation densities used as the objective function to be minimized, effectively integrating equation (4) with the constraints of (6).

2.3. Normal equation lower bound

For this calculation, we begin by mapping the dislocation tensor α into vector form:

$$\alpha_{ij} = \alpha_l, \qquad i=1,3,\ j=1,3,\ \text{and } l=1,9 \tag{7}$$

such that each element of α_l represents a unique element of α_{ij}. With this, we can express equation (4) in the standard form of a linear equation.

$$\alpha_l = A_{lk}\rho_k \qquad l=1,9 \text{ and } k=1,36 \tag{8}$$

where k represents the dislocation system, and each element of the matrix A represents the component (i,j) of the dyadic $b^k \otimes \hat{z}^k$ corresponding to the mapping of (7) from l to i and j. We shall hereafter omit the indices to rewrite relation (8) as $\alpha = A\rho$. Setting $\rho = A^T u$, we then convert the system into a set of normal equations via the method of Kaczmarz [8]:

$$\rho = A^T\left(AA^T\right)^{-1}\alpha \tag{9}$$

Thus, solving for u sets up the direct solution for ρ. Explicitly, (9) represents the set of normal equations for the least squares problem:

$$\textbf{minmize}\left\|\rho^* - A^T u\right\|_2 \tag{10}$$

where ρ* represents any solution to the original underdetermined problem. Since by definition $\rho = A^T u$, equation (10) then finds the set of dislocation densities ρ closest to ρ* in the 2-norm sense. The strength of this method is that it does not artificially limit the number of non-zero dislocation densities to nine as in the Simplex method, which indirectly indicates that only nine dislocations *can* be responsible for the observed dislocation tensor. Rather, it returns the dislocation densities of all thirty-six dislocations with the minimum total density, and as such is believed to be a more accurate representation of a lower-bound solution.

3. Experimental

Cylindrical samples were cut from a directionally solidified, high purity (5N) aluminum ingot. Wire Electrical Discharge Machining was used in order to minimize any deformation that could occur during machining. The samples were cut so their cylindrical axis was parallel to the solidification axis, and the resulting microstructure consisted of long, columnar grains with the <001> crystallographic axis parallel to the columnar direction and diameters between 1 and 3 mm.

The columnar nature of the sample is critical to the experiment in that it permits the critical assumption that the lattice curvature into the characterized plane of the sample is negligible relative to the in-plane curvature: $g_{jl,3} \cong 0$. The principal limitation being addressed with the preparation of columnar microstructures is the electron opacity of crystalline materials, and hence the lack of direct calculation of the in-plane curvature. Given that only components of the form $g_{jl,1}$ and $g_{jl,2}$ are experimentally accessible by electron diffraction, unless $g_{jl,3} = 0$ it is only possible to recover three of the nine components α_{ij} of the dislocation tensor.

Deformation was carried out using uniaxial compression tests at set strain levels, with the compression axis parallel to the cylindrical axis of the sample (and columnar axis of the grains). Specimen preparation was performed on a Logitech PM5 with a $3\mu m$ Alumina lap followed by a $0.02\mu m$ Silica polish. Pressure on the sample was finely controlled in order to ensure that no added deformation was imparted to the sample during the preparation phase.

Following the specimen preparation, spatial crystallographic orientation information was then obtained across high angle grain boundaries using an automated OIM system coupled to a FEGSEM. Orientation information was collected around grain boundaries in a square grid with $500nm$ steps. Typical grid sizes were on the order of 200 x $200\mu m^2$. Using similar methods to those previously reported [9], the accuracy of orientation measurement was found to affect the results reported in the next section by approximately 5%.

4. Results

Datasets obtained from compressed samples were examined in the context described above, and both the lower-bound fcc deconstruction (LB) as well as the normal equation lower-bound fcc deconstruction (NELB) calculations were performed and compared. Fig. 1 below represents a sample dataset across a high angle grain boundary, where the lighter the grayscale the closer the crystallographic <001> is to the surface normal. It is clear that orientation variations in the grain to the right of the boundary are more frequent and more abrupt. It is worth mentioning here that the diameter of the grain to the right of the boundary is approximately $2mm$, while for the grain on the left it is double that at nearly $4mm$, indicating that a size effect may come into play.

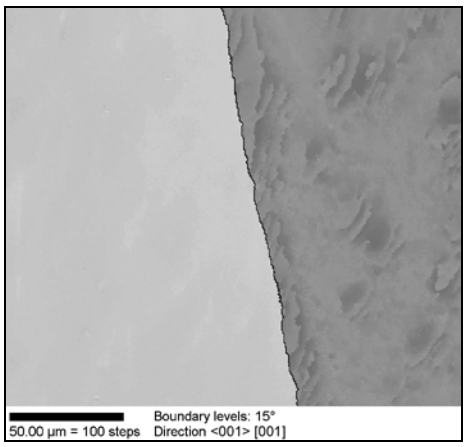

Fig. 1. Crystal orientation plot. Lighter grayscale indicates orientation closer to crystallographic <001>.

In order to calculate the orientation gradient, we first apply all 24 proper symmetry operators to each data point such that the misorientation angle between it and its neighbors is

minimized. This calculation is performed in order to ensure that all the computed orientation gradients were not artificially inflated by taking into account all physically equivalent, yet computationally different, orientations that may arise. Once the orientation gradient, and hence the Nye tensor is calculated, we can plot this as shown in Fig. 2 to get a feel for where the gradients are strongest. The L-2 norm is calculated for the tensor at each point, and the values are normalized such that all values fit between 0 and 1. The orientation gradient across the grain boundary is ignored in this calculation. By comparing Figs. 1 and 2, it is clear that areas with a large amount of lattice curvature seen in Fig. 1 correspond directly to the areas with high orientation gradient in Fig. 2. By applying the techniques described in Sections (2.1-3) to the computed gradient, we can now back out the GND densities

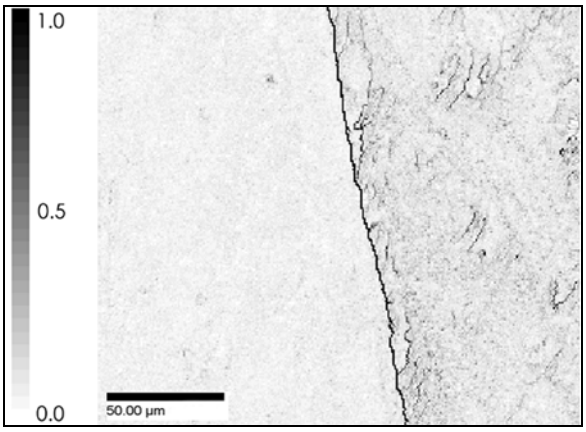

Fig. 2. Normalized L-2 norm of the orientation gradient.

The twelve systems used are defined following Reid [10], and their associated individual dislocations used as input into the LB and NELB calculations. The results of these calculations are shown in the grayscale plots of Fig. 3.

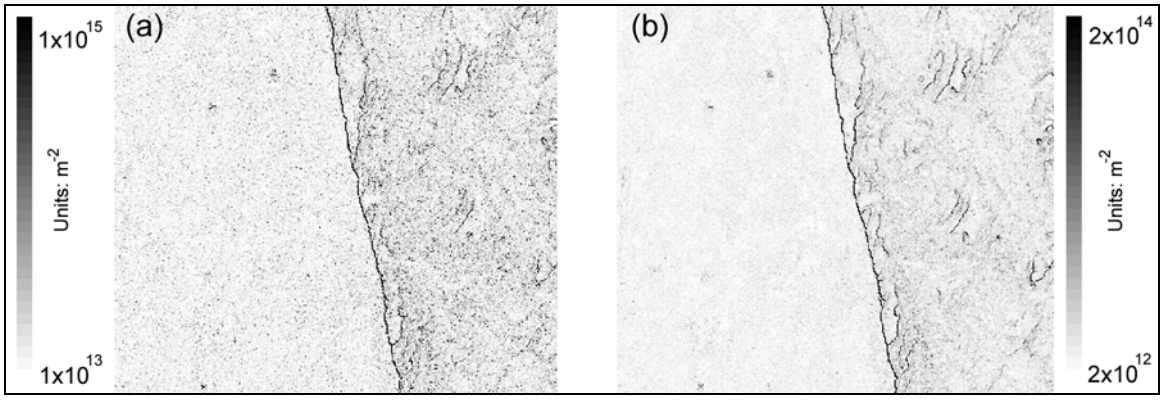

Fig.3. (a) ρ_{GND} estimate using the lower-bound fcc deconstruction (LB) and,
(b) ρ_{GND} estimate using the normal equation lower bound (NELB)

The first apparent difference is in the value of the GND estimate, with the NELB method yielding a maximum ρ_{GND} one-fifth the magnitude of the LB calculation. The second difference is in the grayscale pattern that emerges. Examination shows that the result from the

LB calculation tends to be more "noisy", in that the magnitude of the dislocation densities does not vary as smoothly and on occasion is intermittent when crossing a region with high orientation gradient. In this regard, the NELB method correlates better when compared to the Nye tensor calculation in Fig. 2.

Another important aspect of this comparison is the type of dislocations. Since both calculations return the density for individual dislocations, a correlation between the solutions of both methods can be constructed. The correlation used considers the five slip systems with the highest total dislocation density at each point of both solutions, so that the resultant systems from the LB solution are compared to those from the NELB solution, and a percentage overlap is recorded (*Note:* the number of five systems is chosen for later comparison to the active systems as predicted by Taylor's theory). Repeating this for the whole scan area has yielded a net overlap of 71%. This means that both methods tend to predict the same highly active systems 71% of the time, and the difference may be due to the intermittent quality of the LB solution as discussed above.

5. Summary and Discussion

The overarching trends in the observations of GND pileups near grain boundaries in <001> columnar Aluminum, deformed in compression, are similar to those reported for deformed Aluminum bicrystals [3]: (1) Curvature of the lattice, associated with geometrically-necessary dislocations, tends to accumulate near grain boundaries over distances that extend a substantial fraction (~25%) of the crystallite size (grain size in the present study); and (2) these GND pileups are sensitive to the crystallographic parameters of grain boundary character, and they often present an asymmetrical aspect – with one side carrying much greater curvature than the other.

Reconsideration of the LB methodology, applied in the original work, leads to the conclusion that previous estimates of the required GND densities were over-estimated, although the general trends and length scales remain as reported [3]. The application of normal equations to the recovery algorithm (NELB) has the effect of spreading the curvature over larger sets of GNDs, with the effect of relaxing the overall required densities by a factor of ~5 and thus providing what is believed to be a more representative lower bound ρ_{GND} estimate. The exact nature of this relaxation is not well understood at this time, and in conjunction with other physical aspects of plastic deformation such as the Schmid and Taylor factors pertinent to the imposed deformation, is the subject of current study.

Acknowledgements

The authors wish to thank The Alcoa Technical Research Center for supplying the specimens and performing the compression tests. This work was supported by the MRSEC program of the National Science Foundation under DMR-0079996 as well as Lawrence Livermore Laboratory DOE/DoD Joint Program.

References

[1] G.I.Taylor (1938) J. Inst. Metals 62, 307-315.
[2] N.A.Fleck, G.M.Muller, M.F.Ashby, and J.W.Hutchinson (1994) Acta Metall. Mater. 42, 475.
[3] S.Sun, B.L.Adams, and W.E.King (2000) Phil. Mag. A 80, 9-25.

[4] M.F.Ashby (1970) Phil. Mag. 21, 339.
[5] E.Kroner (1958) Continuum Theory of Dislocations and Self Stresses, Springer-Berlin.
[6] J.F.Nye (1953) Acta Metall. 1, 153.
[7] G.B.Dantzig (1963) Linear Programming and Extensions, Princeton University Press.
[8] S.Kaczmarz (1937) Angenäherte auflösung von systemen linearer gleichungen, Bulletin international de l'Académie polonaise des Sciences et Lettres, 355-357.
[9] M.C.Demirel, B.S.El-Dasher, B.L.Adams, and A.D.Rollett (2000) Electron Backscatter Diffraction in Material Science, (A.J. Schwartz et al, ed.) Kluwer Academic, 65-74.
[10] C.N.Reid (1973) Deformation Geometry for Materials Scientists, Pergamon Press.